Modelling the propagation of infectious disease via transportation networks – Supplementary Information File

Anupriya[1†], Prateek Bansal[2†] and Daniel J. Graham[1*†]

[1*]Transport Strategy Centre, Department of Civil & Environmental Engineering, Imperial College London, London, SW7 2AZ, UK.

[2]Department of Civil and Environmental Engineering, National University of Singapore, Singapore.

*Corresponding author(s). E-mail(s): d.j.graham@imperial.ac.uk;
Contributing authors: anupriya15@imperial.ac.uk;
ceev236@nus.edu.sg;
†These authors contributed equally to this work.

Abstract

This supporting information file is organised as follows. Section 1 illustrates our proposed a risk generation-propagation model. Section 2 gives the expressions for the expansion terms of the zonal propagation potential vector and connectivity propagation metric in unit notations. Section 3 presents a simulation study to evaluate how our proposed inverse connectivity matrix models the potential propagation of infectious disease via transport networks, and to investigate the potential significance of higher-order effects in the propagation process. In the final section, we attach the spatial distributions of estimated transmission risk and observed weekly COVID-19 case incidences in Italy.

1 Infection risk transmission table

Table S.1 illustrates our proposed a risk generation-propagation model that is based on equation 1.

2 Understanding higher-order effects in ICM and CPM

We express the expansion terms, $\boldsymbol{At}$, $\boldsymbol{A}^2\boldsymbol{t}$ and $\boldsymbol{A}^3\boldsymbol{t}$, of the zonal propagation potential vector $\boldsymbol{p}$ in unit notation to illustrate the measure of higher-order effects.

Note that the i^{th} term of the column vector $\boldsymbol{At}$ represents the summation of first-order risk transmission effects from all zones j to i multiplied by the zonal scale of j. Intuitively, this term sums the contribution of infections in each zone j towards the risk of infection in zone i generated via direct importation of infections from zone j to zone i. Similarly, the i^{th} term of of the column vector $\boldsymbol{A}^2\boldsymbol{t}$ represents the summation of second-order risk transmission effects from all zones j to i multiplied by the zonal scale of j. Thus, this term characterises the summation of contribution of infections in each zone j towards the risk of infection in zone i generated through successive propagation of infections from zone j to zone i via zone k.

Similarly, the significance of the CPM estimates can be better understood using their unit notation representations.

3 Simulation

In this section we present a simulation study to evaluate how the ICM models the potential propagation of COVID-19 via transport networks, and specifically, to investigate the potential significance of higher-order effects in the

Table S.1: Infection risk transmission table.

From \ To		Destinations 1	2	3	4	...	n	Total risk originated	Risk imported	Total risk propagated
Origins	1	$x_{11}r_1$	$x_{12}r_1$	$x_{13}r_1$	$x_{14}r_1$	...	$x_{1n}r_1$	$\sum_{j=1}^{n} x_{1j}r_1$	R_{D_1}	p_1
	2	$x_{21}r_2$	$x_{22}r_2$	$x_{23}r_2$	$x_{24}r_2$	...	$x_{2n}r_2$	$\sum_{j=1}^{n} x_{2j}r_2$	R_{D_2}	p_2
	3	$x_{31}r_3$	$x_{32}r_3$	$x_{33}r_3$	$x_{34}r_3$	...	$x_{3n}r_3$	$\sum_{j=1}^{n} x_{3j}r_3$	R_{D_3}	p_3
	4	$x_{41}r_4$	$x_{42}r_4$	$x_{43}r_4$	$x_{44}r_4$	...	$x_{4n}r_4$	$\sum_{j=1}^{n} x_{4j}r_4$	R_{D_4}	p_4
	$\vdots$	$\vdots$	$\vdots$	$\vdots$	$\vdots$	$\ddots$	$\vdots$	$\vdots$	$\vdots$	$\vdots$
	n	$x_{n1}r_n$	$x_{n2}r_n$	$x_{n3}r_n$	$x_{n4}r_n$	...	$x_{nn}r_n$	$\sum_{j=1}^{n} x_{nj}r_n$	R_{D_n}	p_n
Total risk ended		$\sum_{j=1}^{n} x_{j1}r_j$	$\sum_{j=1}^{n} x_{j2}r_j$	$\sum_{j=1}^{n} x_{j3}r_j$	$\sum_{j=1}^{n} x_{j4}r_j$	...	$\sum_{j=1}^{n} x_{jn}r_j$	-	$R_D = \sum_{i=1}^{n} R_{D_i}$	-
Zonal activity scale		R_{O_1}	R_{O_2}	R_{O_3}	R_{O_4}	...	R_{O_n}	$R_O = \sum_{i=1}^{n} R_{O_i}$	-	-
Total risk generated		p_1	p_2	p_3	p_4	...	p_n	-	-	$p = \sum_{i=1}^{n} p_i$

$$
\boldsymbol{CPM} = \begin{bmatrix}
\sum_{j=1}^{n} S_j + \sum_{j=1}^{n} a_{j1} S_j + \sum_{j=1}^{n}\sum_{k=1}^{n} a_{jk}a_{k1} S_j + \sum_{j=1}^{n}\sum_{k=1}^{n}\sum_{l=1}^{n} a_{jk}a_{kl}a_{l1} S_j + \ \dots \\
\sum_{j=1}^{n} S_j + \sum_{j=1}^{n} a_{j2} S_j + \sum_{j=1}^{n}\sum_{k=1}^{n} a_{jk}a_{k2} S_j + \sum_{j=1}^{n}\sum_{k=1}^{n}\sum_{l=1}^{n} a_{jk}a_{kl}a_{l2} S_j + \ \dots \\
\sum_{j=1}^{n} S_j + \sum_{j=1}^{n} a_{j3} S_j + \sum_{j=1}^{n}\sum_{k=1}^{n} a_{jk}a_{k3} S_j + \sum_{j=1}^{n}\sum_{k=1}^{n}\sum_{l=1}^{n} a_{jk}a_{kl}a_{l3} S_j + \ \dots \\
\vdots \\
\sum_{j=1}^{n} S_j + \sum_{j=1}^{n} a_{jn} S_j + \sum_{j=1}^{n}\sum_{k=1}^{n} a_{jk}a_{kn} S_j + \sum_{j=1}^{n}\sum_{k=1}^{n}\sum_{l=1}^{n} a_{jk}a_{kl}a_{ln} S_j + \ \dots
\end{bmatrix}
$$

$$
= \begin{bmatrix}
\sum_{j=1}^{n} S_j + \sum_{j=1}^{n} \frac{x_{1j}r_1}{p_1} S_j + \sum_{j=1}^{n}\sum_{k=1}^{n} \frac{x_{1k}r_1}{p_1}\frac{x_{kj}r_k}{p_k} S_j + \sum_{j=1}^{n}\sum_{k=1}^{n}\sum_{l=1}^{n} \frac{x_{1l}r_1}{p_1}\frac{x_{lk}r_l}{p_l}\frac{x_{kj}r_k}{p_k} S_j + \ \dots \\
\sum_{j=1}^{n} S_j + \sum_{j=1}^{n} \frac{x_{2j}r_2}{p_2} S_j + \sum_{j=1}^{n}\sum_{k=1}^{n} \frac{x_{2k}r_2}{p_2}\frac{x_{kj}r_k}{p_k} S_j + \sum_{j=1}^{n}\sum_{k=1}^{n}\sum_{l=1}^{n} \frac{x_{2l}r_2}{p_2}\frac{x_{lk}r_l}{p_l}\frac{x_{kj}r_k}{p_k} S_j + \ \dots \\
\sum_{j=1}^{n} S_j + \sum_{j=1}^{n} \frac{x_{3j}r_3}{p_3} S_j + \sum_{j=1}^{n}\sum_{k=1}^{n} \frac{x_{3k}r_3}{p_3}\frac{x_{kj}r_k}{p_k} S_j + \sum_{j=1}^{n}\sum_{k=1}^{n}\sum_{l=1}^{n} \frac{x_{3l}r_3}{p_3}\frac{x_{lk}r_l}{p_l}\frac{x_{kj}r_k}{p_k} S_j + \ \dots \\
\vdots \\
\sum_{j=1}^{n} S_j + \sum_{j=1}^{n} \frac{x_{nj}r_n}{p_n} S_j + \sum_{j=1}^{n}\sum_{k=1}^{n} \frac{x_{nk}r_n}{p_n}\frac{x_{kj}r_k}{p_k} S_j + \sum_{j=1}^{n}\sum_{k=1}^{n}\sum_{l=1}^{n} \frac{x_{nl}r_n}{p_n}\frac{x_{lk}r_l}{p_l}\frac{x_{kj}r_k}{p_k} S_j + \ \dots
\end{bmatrix}
$$

$$\boldsymbol{At} = \begin{bmatrix} \sum_{j=1}^{n} a_{1j} t_j = \sum_{j=1}^{n} \frac{x_{j1} r_j}{p_j} t_j \\ \sum_{j=1}^{n} a_{2j} t_j = \sum_{j=1}^{n} \frac{x_{j2} r_j}{p_j} t_j \\ \sum_{j=1}^{n} a_{3j} t_j = \sum_{j=1}^{n} \frac{x_{j3} r_j}{p_j} t_j \\ \vdots \\ \sum_{j=1}^{n} a_{4j} t_j = \sum_{j=1}^{n} \frac{x_{jn} r_j}{p_j} t_j \end{bmatrix};$$

$$\boldsymbol{A}^2\boldsymbol{t} = \begin{bmatrix} \sum_{j=1}^{n} a_{1k} a_{kj} t_j \sum_{j=1}^{n} \sum_{k=1}^{n} \frac{x_{jk} r_j}{p_j} \frac{x_{k1} r_k}{p_k} t_j \\ \sum_{j=1}^{n} a_{2k} a_{kj} t_j \sum_{j=1}^{n} \sum_{k=1}^{n} \frac{x_{jk} r_j}{p_j} \frac{x_{k2} r_k}{p_k} t_j \\ \sum_{j=1}^{n} a_{3k} a_{kj} t_j \sum_{j=1}^{n} \sum_{k=1}^{n} \frac{x_{jk} r_j}{p_j} \frac{x_{k3} r_k}{p_k} t_j \\ \vdots \\ \sum_{j=1}^{n} a_{nk} a_{kj} t_j \sum_{j=1}^{n} \sum_{k=1}^{n} \frac{x_{jk} r_j}{p_j} \frac{x_{kn} r_k}{p_k} t_j \end{bmatrix};$$

$$\boldsymbol{A}^3\boldsymbol{t} = \begin{bmatrix} \sum_{j=1}^{n} a_{1l} a_{lk} a_{kj} t_j = \sum_{j=1}^{n} \sum_{k=1}^{n} \sum_{l=1}^{n} \frac{x_{jk} r_j}{p_j} \frac{x_{kl} r_k}{p_k} \frac{x_{l1} r_l}{p_l} t_j \\ \sum_{j=1}^{n} a_{2l} a_{lk} a_{kj} t_j = \sum_{j=1}^{n} \sum_{k=1}^{n} \sum_{l=1}^{n} \frac{x_{jk} r_j}{p_j} \frac{x_{kl} r_k}{p_k} \frac{x_{l2} r_l}{p_l} t_j \\ \sum_{j=1}^{n} a_{3l} a_{lk} a_{kj} t_j = \sum_{j=1}^{n} \sum_{k=1}^{n} \sum_{l=1}^{n} \frac{x_{jk} r_j}{p_j} \frac{x_{kl} r_k}{p_k} \frac{x_{l3} r_l}{p_l} t_j \\ \vdots \\ \sum_{j=1}^{n} a_{nl} a_{lk} a_{kj} t_j = \sum_{j=1}^{n} \sum_{k=1}^{n} \sum_{l=1}^{n} \frac{x_{jk} r_j}{p_j} \frac{x_{kl} r_k}{p_k} \frac{x_{ln} r_l}{p_l} t_j \end{bmatrix}; \quad \text{and so on.}$$

propagation process. We consider a transportation network comprising one hundred zones, each indexed by i, $i = (1, ..., 100)$, with a layout as shown in Figure S.2a. The population of each zone is drawn from a log-normal distribution with mean 1000 and standard deviation 800. To simulate the corresponding OD matrix, we adopt the radiation model for human mobility [1]. This model is widely known to best approximate the observed distribution of real-world long-distance trips. The fundamental equation of the radiation model quantifies the average flux or trips, X_{ij}, from zone i to zone j:

$$X_{ij} = X_i \times \frac{m_i \times n_j}{(m_i + s_{ij})(m_i + n_j + s_{ij})} \tag{S.1}$$

where X_i is the total number of travellers from zone i, m_i and n_j are the population in zone i and j respectively, and s_{ij} is the total population in the circle centered at i and touching j excluding the source and the destination population. We generate the values of X_i, that is, the total number of travellers from zone i, by assuming the proportion of travellers in each zone to be uniformly distributed in a range [0.5,1]. For the purpose of this simulation, we set both the risk r_i and susceptibility s_i of each zone i as 1. After generating the risk matrix with terms $r_i X_{ij} = X_{ij}$, we estimate other quantities (t vector, p vector, A matrix, ICM, and CPM vector) as explained in Section 2.

To understand the contribution of higher order transport connectivity effects towards the zonal propagation potential p, we obtain approximate estimates of p (that is, $(\boldsymbol{I} - \boldsymbol{A})^{-1} t$) by iteratively adding one higher-order term at a time. At each iteration l, we estimate p using equation S.2.

$$p = (\boldsymbol{I} - \boldsymbol{A})^{-1} \boldsymbol{t} = \sum_{r=0}^{l} \boldsymbol{A}^r \boldsymbol{t} \tag{S.2}$$

We record the euclidean distance between the observed p and the approximated p at each iteration. Figure S.2b plots these euclidean distance values over the number of higher order terms included in the approximation. This figure illustrates that higher order effects up to the fifth degree contribute significantly to the observed total propagation potential of the system. Note that

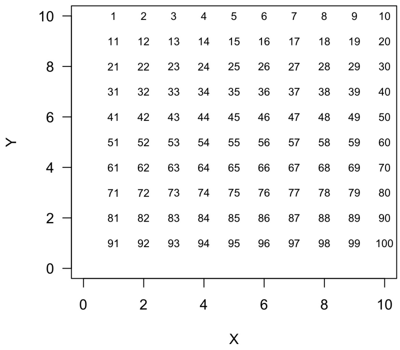

(a) Zonal layout.

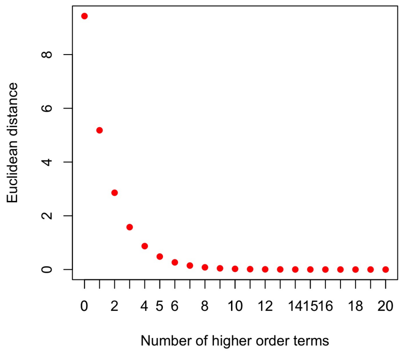

(b) Significance of higher order connectivity effects.

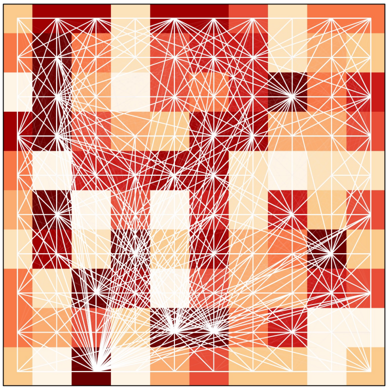

(c) A heat map of the zonal population with top ten percentile of risk flows.

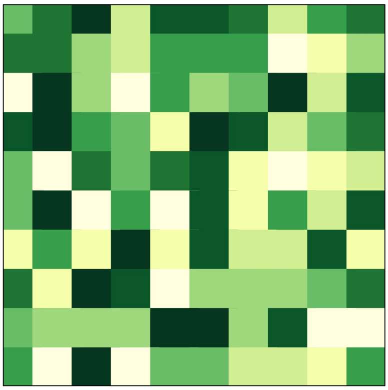

(d) A heat map of the connectivity propagation metric (CPM) times the zonal activity scale (t).

Fig. S.2: A simulation study to demonstrate the potential propagation of COVID-19 via transportation network connectivity.

the importance of higher-order effects inherently depends on the data generating process of the empirical study and can vary across applications and geographical settings.

Figure S.2c shows a heat map of the zonal population with the top ten percentile of risk flows (that is, $r_i X_{ij} = X_{ij}$). Figure S.2d shows the corresponding heat map of the $CPM \times t$ metric. We scale the CPM estimates by their corresponding t to understand the impact of all interactions from the zone. We note that zones with higher intensity of flows are by and large associated with a higher $CPM \times t$ value. Note that figure S.2c shows only the first-order propagation via transport network connectivity and does not include any higher-order effects, so there may not be one-to-one correspondence between the figures. Based on this figure, we conclude that the higher the $CPM \times t$ value for a zone, the higher is the number and intensity (that is, proportion of trips) of connections between the zone and with the entire system and as a result, the higher will be the impact of interactions from the zone on the entire system. Because by definition these zonal interactions indicate the risk of infections originating in the zone, we can use this setup to model the risk of propagation of infectious diseases like COVID-19 through transport networks.

4 Full Results

Figures S.3 to S.14 show the spatial distributions of estimated transmission risk and observed weekly COVID-19 case incidences in Italy during our study period.

References

[1] Simini, F., González, M.C., Maritan, A., Barabási, A.-L.: A universal model for mobility and migration patterns. Nature **484**(7392), 96–100 (2012)

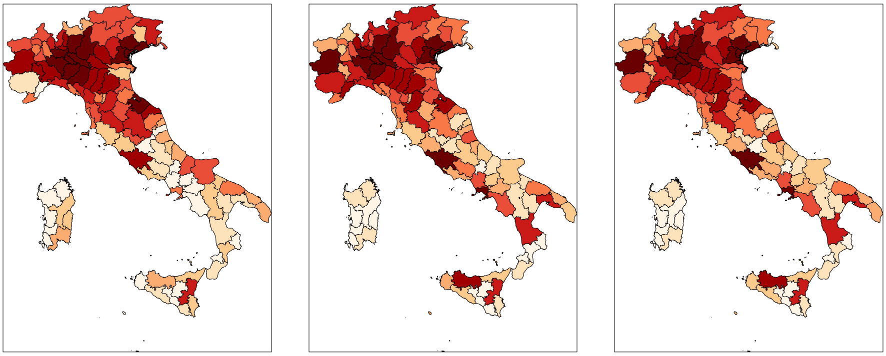

(a) A heatmap of observed cases.

(b) A heatmap of transmission risk estimated via both first and higher connectivity effects [$r_s = 0.7110$].

(c) A heatmap of transmission risk estimated via first-order connectivity effects [$r_s = 0.7062$].

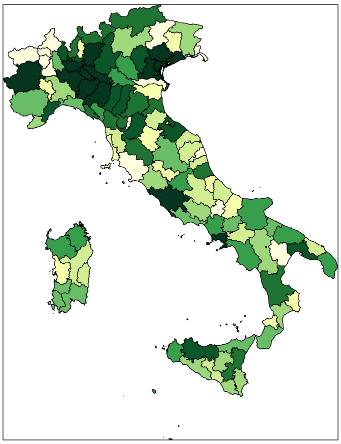

(d) A heatmap of estimated connectivity propagation metric times active case load.

Name of the province	Rank (by CPM× active cases)
Lodi	1
Bergamo	2
Milano	3
Cremona	4
Padova	5
Piacenza	6
Pavia	7
Napoli	8
Treviso	9
Roma	10
Torino	11
Parma	12
Venezia	13
Brescia	14
Modena	15
Savona	16
Monza e della Brianza	17
Rimini	18
Firenze	19
Varese	20

(e) List of top twenty provinces for likely intervention.

Fig. S.3: Spatial distributions of estimated transmission risk and observed new COVID-19 cases in the week ending 7 March 2020.

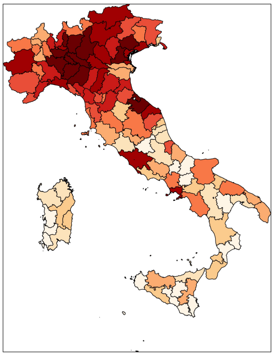

(a) A heatmap of observed cases.

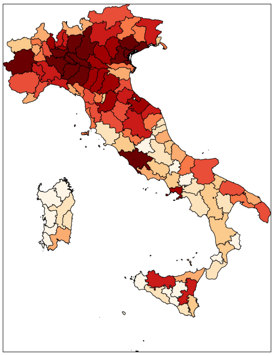

(b) A heatmap of transmission risk estimated via both first and higher connectivity effects [$r_s = 0.8857$].

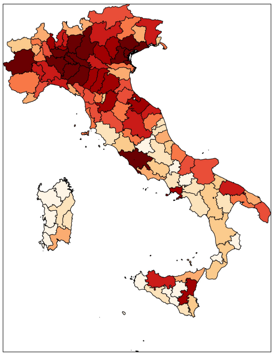

(c) A heatmap of transmission risk estimated via first-order connectivity effects [$r_s = 0.8787$].

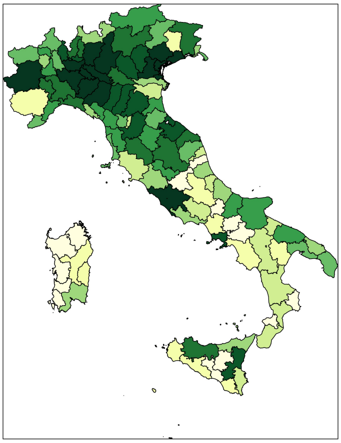

(d) A heatmap of estimated connectivity propagation metric times active case load.

Name of the province	Rank (by CPM× active cases)
Milano	1
Bergamo	2
Lodi	3
Brescia	4
Cremona	5
Roma	6
Padova	7
Pavia	8
Piacenza	9
Torino	10
Parma	11
Treviso	12
Venezia	13
Pesaro E Urbino	14
Monza e della Brianza	15
Modena	16
Napoli	17
Verona	18
Bologna	19
Rimini	20

(e) List of top twenty provinces for likely intervention.

Fig. S.4: Spatial distributions of estimated transmission risk and observed new COVID-19 cases in the week ending 14 March 2020.

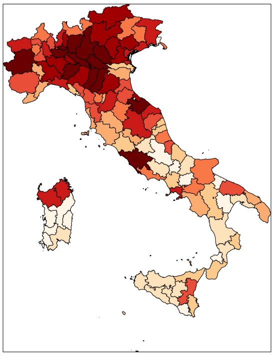

(a) A heatmap of observed cases.

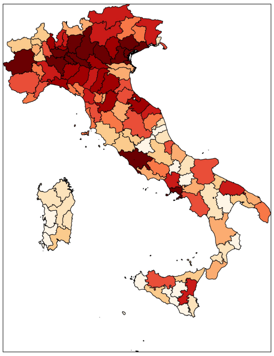

(b) A heatmap of transmission risk estimated via both first and higher connectivity effects [$r_s = 0.8705$].

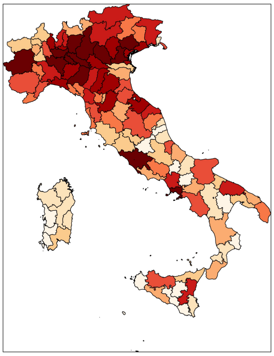

(c) A heatmap of transmission risk estimated via first-order connectivity effects [$r_s = 0.8683$].

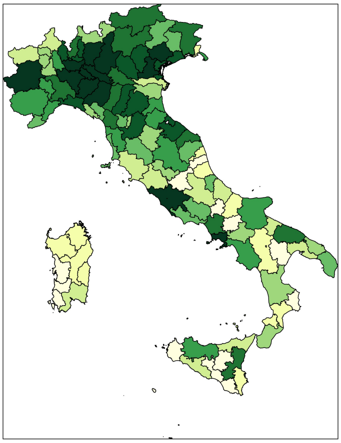

(d) A heatmap of estimated connectivity propagation metric times active case load.

Name of the province	Rank (by CPM× active cases)
Milano	1
Bergamo	2
Brescia	3
Roma	4
Cremona	5
Torino	6
Lodi	7
Padova	8
Napoli	9
Pavia	10
Treviso	11
Piacenza	12
Parma	13
Verona	14
Venezia	15
Pesaro E Urbino	16
Modena	17
Monza e della Brianza	18
Genova	19
Bologna	20

(e) List of top twenty provinces for likely intervention.

Fig. S.5: Spatial distributions of estimated transmission risk and observed new COVID-19 cases in the week ending 21 March 2020.

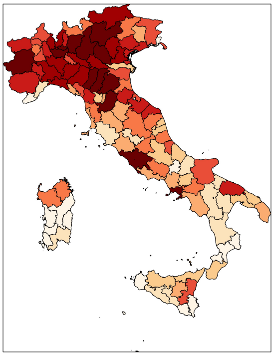

(a) A heatmap of observed cases.

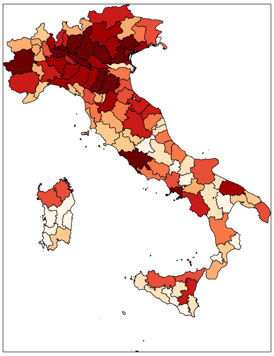

(b) A heatmap of transmission risk estimated via both first and higher connectivity effects [$r_s = 0.8988$].

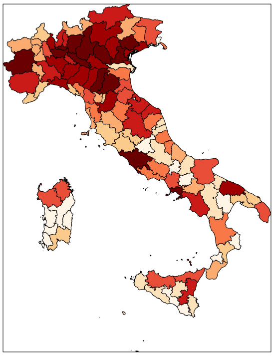

(c) A heatmap of transmission risk estimated via first-order connectivity effects [$r_s = 0.8992$].

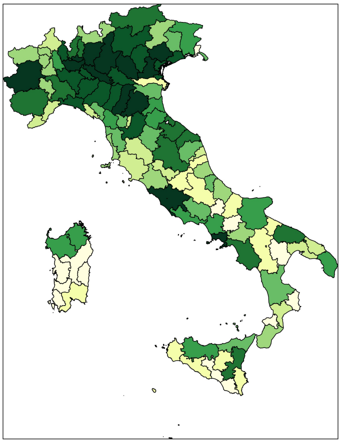

(d) A heatmap of estimated connectivity propagation metric times active case load.

Name of the province	Rank (by CPM× active cases)
Milano	1
Brescia	2
Bergamo	3
Torino	4
Roma	5
Napoli	6
Monza e della Brianza	7
Padova	8
Verona	9
Cremona	10
Bologna	11
Modena	12
Treviso	13
Pavia	14
Reggio Nell'Emilia	15
Vicenza	16
Venezia	17
Firenze	18
Trento	19
Parma	20

(e) List of top twenty provinces for likely intervention.

Fig. S.6: Spatial distributions of estimated transmission risk and observed new COVID-19 cases in the week ending 4 April 2020.

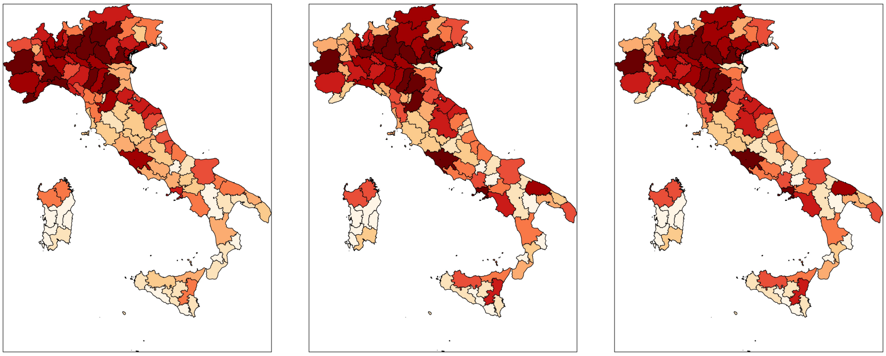

(a) A heatmap of observed cases.

(b) A heatmap of transmission risk estimated via both first and higher connectivity effects [$r_s = 0.8268$].

(c) A heatmap of transmission risk estimated via first-order connectivity effects [$r_s = 0.8271$].

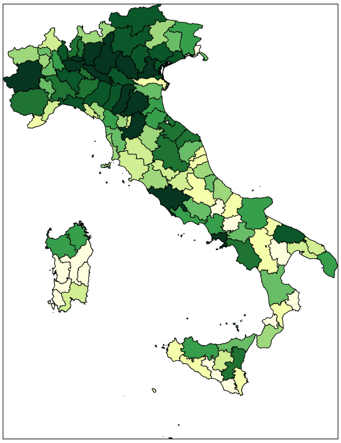

(d) A heatmap of estimated connectivity propagation metric times active case load.

Name of the province	Rank (by CPM× active cases)
Milano	1
Torino	2
Brescia	3
Roma	4
Bergamo	5
Napoli	6
Monza e della Brianza	7
Padova	8
Bologna	9
Verona	10
Modena	11
Cremona	12
Firenze	13
Reggio Nell'Emilia	14
Pavia	15
Treviso	16
Vicenza	17
Trento	18
Venezia	19
Varese	20

(e) List of top twenty provinces for likely intervention.

Fig. S.7: Spatial distributions of estimated transmission risk and observed new COVID-19 cases in the week ending 11 April 2020.

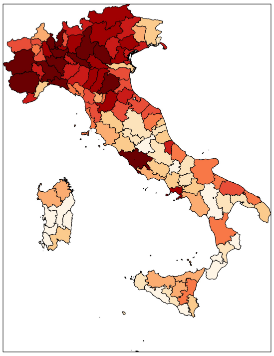

(a) A heatmap of observed cases.

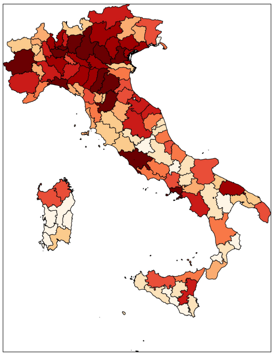

(b) A heatmap of transmission risk estimated via both first and higher connectivity effects [$r_s = 0.8535$].

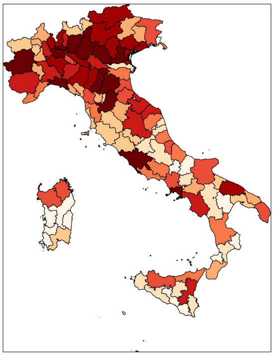

(c) A heatmap of transmission risk estimated via first-order connectivity effects [$r_s = 0.8532$].

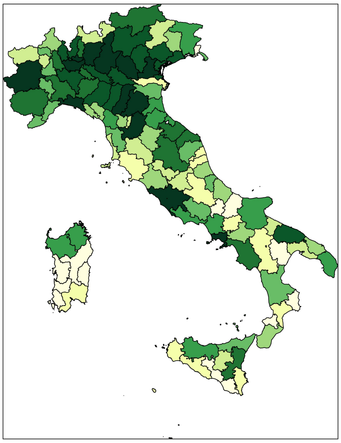

(d) A heatmap of estimated connectivity propagation metric times active case load.

Name of the province	Rank (by CPM× active cases)
Milano	1
Torino	2
Roma	3
Brescia	4
Bergamo	5
Napoli	6
Monza e della Brianza	7
Verona	8
Bologna	9
Padova	10
Genova	11
Firenze	12
Modena	13
Reggio Nell'Emilia	14
Cremona	15
Pavia	16
Treviso	17
Vicenza	18
Venezia	19
Trento	20

(e) List of top twenty provinces for likely intervention.

Fig. S.8: Spatial distributions of estimated transmission risk and observed new COVID-19 cases in the week ending 18 April 2020.

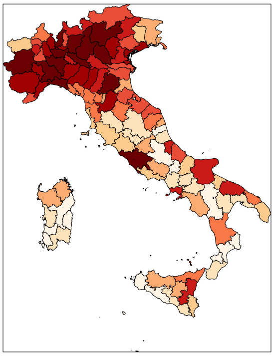

(a) A heatmap of observed cases.

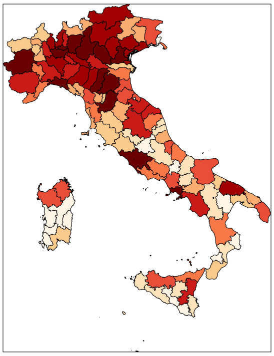

(b) A heatmap of transmission risk estimated via both first and higher connectivity effects [$r_s = 0.8386$].

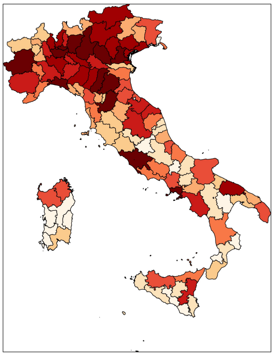

(c) A heatmap of transmission risk estimated via first-order connectivity effects [$r_s = 0.8406$].

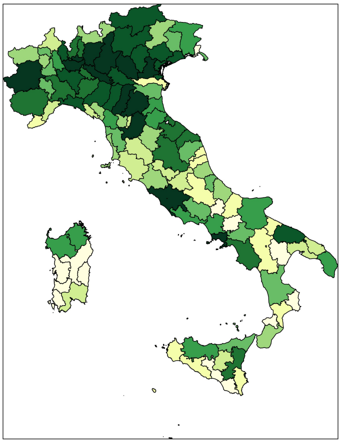

(d) A heatmap of estimated connectivity propagation metric times active case load.

Name of the province	Rank (by CPM× active cases)
Milano	1
Torino	2
Roma	3
Brescia	4
Bergamo	5
Napoli	6
Monza e della Brianza	7
Bologna	8
Verona	9
Padova	10
Genova	11
Firenze	12
Cremona	13
Modena	14
Reggio Nell'Emilia	15
Pavia	16
Treviso	17
Varese	18
Vicenza	19
Trento	20

(e) List of top twenty provinces for likely intervention.

Fig. S.9: Spatial distributions of estimated transmission risk and observed new COVID-19 cases in the week ending 25 April 2020.

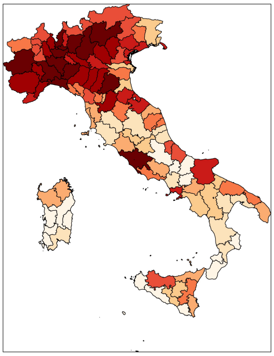

(a) A heatmap of observed cases.

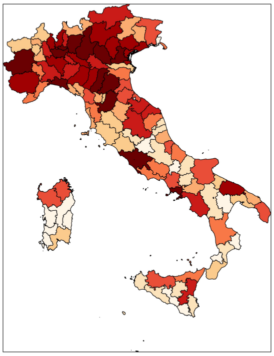

(b) A heatmap of transmission risk estimated via both first and higher connectivity effects [$r_s = 0.8504$].

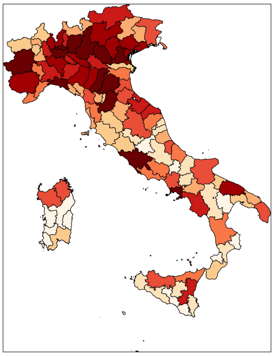

(c) A heatmap of transmission risk estimated via first-order connectivity effects [$r_s = 0.8533$].

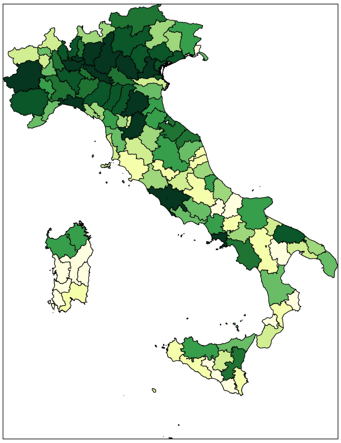

(d) A heatmap of estimated connectivity propagation metric times active case load.

Name of the province	Rank (by CPM× active cases)
Milano	1
Torino	2
Roma	3
Brescia	4
Bergamo	5
Napoli	6
Monza e della Brianza	7
Verona	8
Bologna	9
Padova	10
Genova	11
Firenze	12
Cremona	13
Pavia	14
Reggio Nell'Emilia	15
Modena	16
Varese	17
Treviso	18
Vicenza	19
Trento	20

(e) List of top twenty provinces for likely intervention.

Fig. S.10: Spatial distributions of estimated transmission risk and observed new COVID-19 cases in the week ending 2 May 2020.

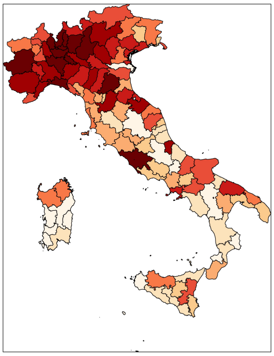

(a) A heatmap of observed cases.

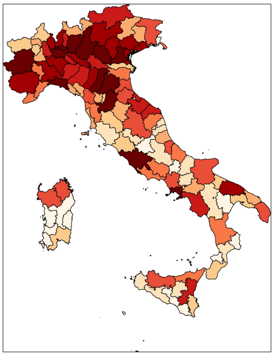

(b) A heatmap of transmission risk estimated via both first and higher connectivity effects [$r_s = 0.8227$].

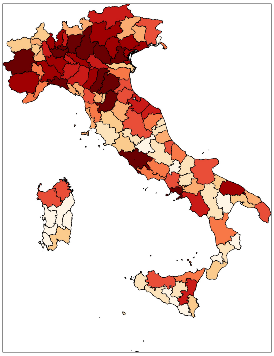

(c) A heatmap of transmission risk estimated via first-order connectivity effects [$r_s = 0.8223$].

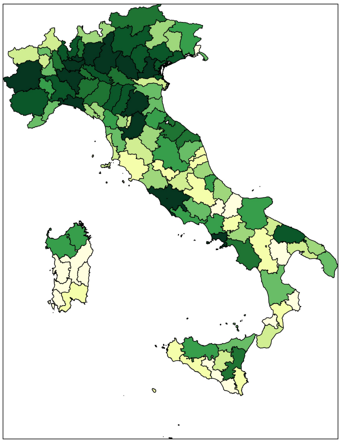

(d) A heatmap of estimated connectivity propagation metric times active case load.

Name of the province	Rank (by CPM× active cases)
Milano	1
Torino	2
Roma	3
Brescia	4
Bergamo	5
Napoli	6
Monza e della Brianza	7
Bologna	8
Verona	9
Genova	10
Padova	11
Firenze	12
Pavia	13
Cremona	14
Varese	15
Modena	16
Reggio Nell'Emilia	17
Vicenza	18
Treviso	19
Trento	20

(e) List of top twenty provinces for likely intervention.

Fig. S.11: Spatial distributions of estimated transmission risk and observed new COVID-19 cases in the week ending 9 May 2020.

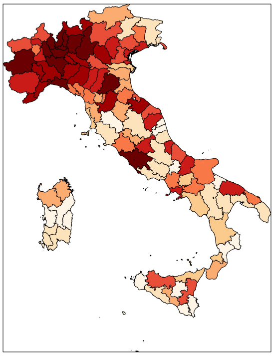

(a) A heatmap of observed cases.

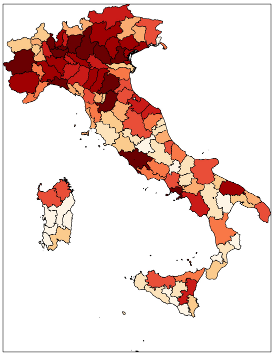

(b) A heatmap of transmission risk estimated via both first and higher connectivity effects [$r_s = 0.7882$].

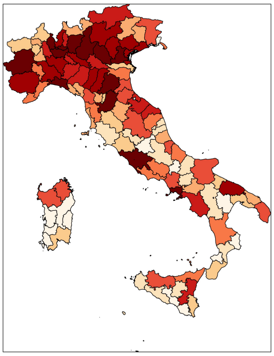

(c) A heatmap of transmission risk estimated via first-order connectivity effects [$r_s = 0.7891$].

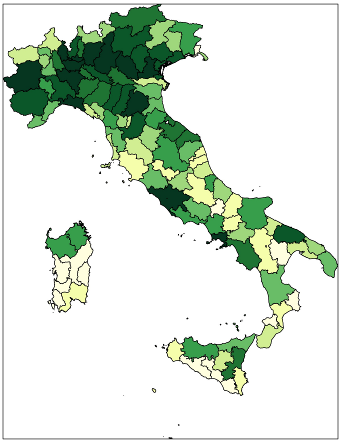

(d) A heatmap of estimated connectivity propagation metric times active case load.

Name of the province	Rank (by CPM× active cases)
Milano	1
Torino	2
Roma	3
Brescia	4
Bergamo	5
Napoli	6
Monza e della Brianza	7
Bologna	8
Verona	9
Genova	10
Padova	11
Varese	12
Pavia	13
Firenze	14
Cremona	15
Reggio Nell'Emilia	16
Modena	17
Como	18
Vicenza	19
Treviso	20

(e) List of top twenty provinces for likely intervention.

Fig. S.12: Spatial distributions of estimated transmission risk and observed new COVID-19 cases in the week ending 16 May 2020.

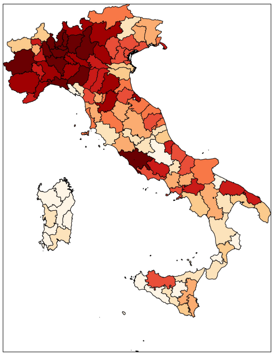

(a) A heatmap of observed cases.

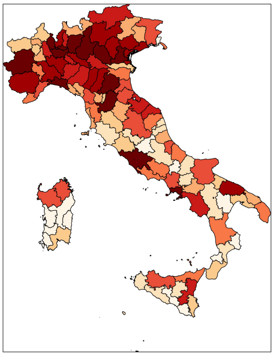

(b) A heatmap of transmission risk estimated via both first and higher connectivity effects [$r_s = 0.7791$].

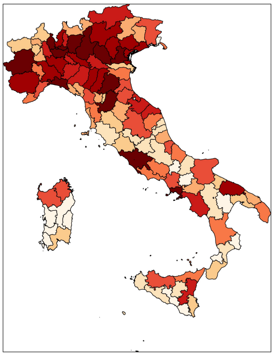

(c) A heatmap of transmission risk estimated via first-order connectivity effects [$r_s = 0.7768$].

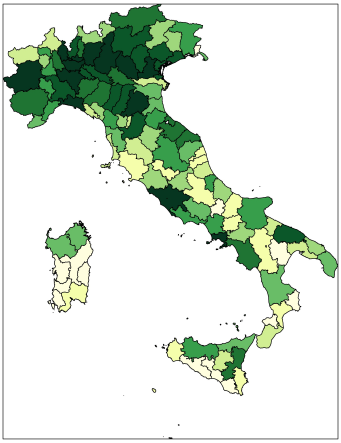

(d) A heatmap of estimated connectivity propagation metric times active case load.

Name of the province	Rank (by CPM× active cases)
Milano	1
Torino	2
Roma	3
Brescia	4
Bergamo	5
Napoli	6
Monza e della Brianza	7
Bologna	8
Verona	9
Genova	10
Padova	11
Varese	12
Pavia	13
Firenze	14
Cremona	15
Reggio Nell'Emilia	16
Modena	17
Como	18
Vicenza	19
Treviso	20

(e) List of top twenty provinces for likely intervention.

Fig. S.13: Spatial distributions of estimated transmission risk and observed new COVID-19 cases in the week ending 23 May 2020.

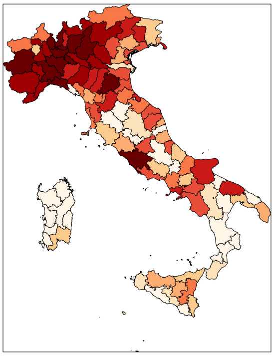

(a) A heatmap of observed cases.

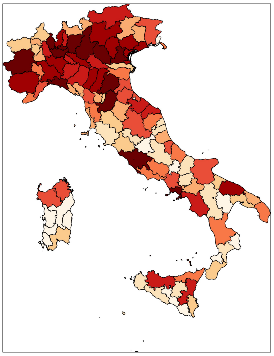

(b) A heatmap of transmission risk estimated via both first and higher connectivity effects [$r_s = 0.7665$].

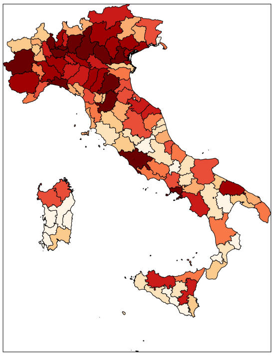

(c) A heatmap of transmission risk estimated via first-order connectivity effects [$r_s = 0.7656$].

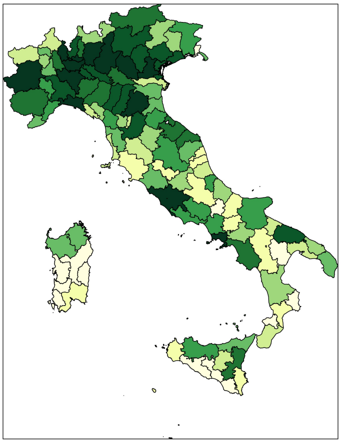

(d) A heatmap of estimated connectivity propagation metric times active case load.

Name of the province	Rank (by CPM× active cases)
Milano	1
Torino	2
Roma	3
Brescia	4
Bergamo	5
Napoli	6
Monza e della Brianza	7
Bologna	8
Verona	9
Genova	10
Pavia	11
Varese	12
Padova	13
Cremona	14
Firenze	15
Como	16
Reggio Nell'Emilia	17
Modena	18
Vicenza	19
Treviso	20

(e) List of top twenty provinces for likely intervention.

Fig. S.14: Spatial distributions of estimated transmission risk and observed new COVID-19 cases in the week ending 30 May 2020.